

## **DISCLAIMER**

**This report was prepared as an account of work sponsored by an agency of the United States Government. Neither the United States Government nor any agency thereof, nor any of their employees, makes any warranty, express or implied, or assumes any legal liability or responsibility for the accuracy, completeness, or usefulness of any information, apparatus, product, or process disclosed, or represents that its use would not infringe privately owned rights. Reference herein to any specific commercial product, process, or service by trade name, trademark, manufacturer, or otherwise does not necessarily constitute or imply its endorsement, recommendation, or favoring by the United States Government or any agency thereof. The views and opinions of authors expressed herein do not necessarily state or reflect those of the United States Government or any agency thereof. Reference herein to any social initiative (including but not limited to Diversity, Equity, and Inclusion (DEI); Community Benefits Plans (CBP); Justice 40; etc.) is made by the Author independent of any current requirement by the United States Government and does not constitute or imply endorsement, recommendation, or support by the United States Government or any agency thereof.**



# Expansion of the Fuel Motion Monitoring System

September 2024

*Changing the World's Energy Future*

Luis A Ocampo Giraldo, David L Chichester, Scott J Thompson, James T Johnson, Jay D Hix, Melissa Jean Daw



**DISCLAIMER**

This information was prepared as an account of work sponsored by an agency of the U.S. Government. Neither the U.S. Government nor any agency thereof, nor any of their employees, makes any warranty, expressed or implied, or assumes any legal liability or responsibility for the accuracy, completeness, or usefulness, of any information, apparatus, product, or process disclosed, or represents that its use would not infringe privately owned rights. References herein to any specific commercial product, process, or service by trade name, trade mark, manufacturer, or otherwise, does not necessarily constitute or imply its endorsement, recommendation, or favoring by the U.S. Government or any agency thereof. The views and opinions of authors expressed herein do not necessarily state or reflect those of the U.S. Government or any agency thereof.

# **Expansion of the Fuel Motion Monitoring System**

**Luis A Ocampo Giraldo, David L Chichester, Scott J Thompson, James T Johnson, Jay D Hix, Melissa Jean Daw**

**September 2024**

**Idaho National Laboratory  
Idaho Falls, Idaho 83415**

**<http://www.inl.gov>**

**Prepared for the  
U.S. Department of Energy  
Under DOE Idaho Operations Office  
Contract DE-AC07-05ID14517**

# Expansion of the Fuel Motion Monitoring System

Applied Radiation Measurements and Systems Group

---

SEPTEMBER 2024

---

David Chichester, Jeffrey Burggraf,  
Melissa Daw, Jay Hix, Tommy Holschuh,  
James Johnson, Luis Ocampo Giraldo,  
Scott Thompson, and Alexis Vega Galaviz

*Idaho National Laboratory*



**DISCLAIMER**

This information was prepared as an account of work sponsored by an agency of the U.S. Government. Neither the U.S. Government nor any agency thereof, nor any of their employees, makes any warranty, expressed or implied, or assumes any legal liability or responsibility for the accuracy, completeness, or usefulness, of any information, apparatus, product, or process disclosed, or represents that its use would not infringe privately owned rights. References herein to any specific commercial product, process, or service by trade name, trade mark, manufacturer, or otherwise, does not necessarily constitute or imply its endorsement, recommendation, or favoring by the U.S. Government or any agency thereof. The views and opinions of authors expressed herein do not necessarily state or reflect those of the U.S. Government or any agency thereof.

# **Expansion of the Fuel Motion Monitoring System**

**Applied Radiation Measurements and Systems Group**

**David Chichester, Jeffrey Burggraf,  
Melissa Daw, Jay Hix, Tommy Holschuh,  
James Johnson, Luis Ocampo Giraldo,  
Scott Thompson, and Alexis Vega Galaviz  
Idaho National Laboratory**

**September 2024**

**Idaho National Laboratory  
Nuclear Nonproliferation Division  
Idaho Falls, Idaho 83415**

**<http://www.inl.gov>**

**Prepared for the  
U.S. Department of Energy  
Nuclear Science User Facilities  
Under DOE Idaho Operations Office  
Contract DE-AC07-05ID14517**

*Page intentionally left blank*

# CONTENTS

ACRONYMS .....	vii
INTRODUCTION .....	1
FUEL MOTION MONITORING SYSTEM .....	1
Heating Issues .....	2
Laboratory Testing .....	4
Voltage Bias .....	5
Detector Count Rates .....	5
Efficiency Measurements .....	9
Absolute Efficiency .....	11
SYSTEM INSTALLATION .....	11
Environmental Monitoring .....	16
SYSTEM TESTING .....	17
Data Acquisition Synchronized Timing .....	18
Transient Reporting .....	19
ACKNOWLEDGEMENTS .....	19
REFERENCES .....	<b>Error! Bookmark not defined.</b>
Appendix A Transient Pulse Summary Report .....	21

## FIGURES

Figure 1. Cross-sectional illustration of the Fuel Motion Monitoring System components.....	2
Figure 2. Hodoscope detector components including the proton recoil scintillator (in white) coupled to the photomultiplier tube.....	2
Figure 3. TRIPP-LITE cooler, shown on the left side, installed into the DAQ cabinet. ....	3
Figure 4. DAQ electronics temperatures after optimization of cooler placement. The centermost image demonstrates the cyclical cooling. ....	4
Figure 5. Mock FMMS testing cabinet. ....	4
Figure 6. Scanning setup with translation stages and radioactive source (left) detector locations used in the mock FMMS testing cabinet (right). ....	5
Figure 7. Results from the bias voltage scan (left). Minimum voltage values to power the detectors (right). ....	5
Figure 8. Detector count rate measurement setup using five neutron sources.....	6
Figure 9. Total distribution of the source normalization .....	7
Figure 10. Voltage bias scan results for 135 detectors using the expanded acquisition system. ....	7
Figure 11. Count rate distribution after the automated normalization of the 135 detectors. ....	8
Figure 12. Illustration of the FOM components used in Eq. 1. ....	8
Figure 13. Detector Figure of Merit (FOM) examples: FOM greater than one (left) and FOM less than one (right). ....	8
Figure 14. Example time of flight spectrum for a FMMS detector assembly. ....	9
Figure 15. Relative neutron efficiency for the evaluated detectors. ....	10
Figure 16. Mean pulse height comparison of hodoscope detectors and the start stilbene detector.....	10
Figure 17. Absolute neutron efficiency for the five evaluated detectors. ....	11
Figure 18. Disconnecting of the cables and removal of the detectors (left). Placement of the new 100-foot cables (right). ....	12
Figure 19. Visual inspection of PRS components .....	12
Figure 20. Photographs of clean PRS (left) and PMT (right) components.....	12
Figure 21. FOM comparison between the new 192 detectors and the original 96 FMMS detectors. ....	13
Figure 22. Comparison of the original FMMS coverage area (left) and the new (right). ....	13
Figure 23. Photograph of the new installed detectors connected to their respective cables. ....	14
Figure 24. Placement of signal and high voltage cables inside the trench. ....	14
Figure 25. Verification scan with the new FMMS DAQ and new detectors. ....	15

Figure 26. Neutron count rate distribution of the baseline scan using the new 192 detectors and DAQ.....	15
Figure 27. Results of the verification scan to verify each detector's parameters. ....	16
Figure 28. FMMS chassis with all new components, the environmental monitor hub (red) is located in the middle. ....	17
Figure 29. RoomAlert32S graphic user interface. ....	17
Figure 30. Cumulative number of counts after the 80 kW .....	18
Figure 31. Example of Struck card drift over several days.....	19

*Page intentionally left blank*

## ACRONYMS

ARMS	Applied Radiation Measurements & Systems
ATR	Advanced Test Reactor
DAQ	Data Acquisition
DOE	U.S. Department of Energy
DOE-ID	U.S. Department of Energy-Idaho Operations Office
FMMS	Fuel Motion Monitoring System
INL	Idaho National Laboratory
MFC	Materials and Fuels Complex
PMT	Photomultiplier Tube
PRS	Proton Recoil Scintillator
R&D	research and development
ToF	Time-of-Flight

*Page intentionally left blank*

# **Expansion of the Fuel Motion Monitoring System**

## **Applied Radiation Measurements and Systems**

### **INTRODUCTION**

The Idaho National Laboratory (INL) Transient Reactor Test Facility (TREAT) Fuel Motion Monitoring System (FMMS) is a diagnostic tool used to visualize the movement and location of fuel within the nuclear reactor during transient experiments. TREAT is designed to test the behavior of nuclear fuel under accident conditions, such as a rapid power increase. The TREAT FMMS, also referred to as the “hodoscope” because of the system’s massive steel collimator component, is located on the North beam port of the reactor. While the FMMS system is capable of incorporating a total of 360 sensors, initial refurbishment efforts resulted in a array of 96 fast neutron detectors. This initial array was configured to provide a narrow (2 channels) full-length view of experiment vessels with an extended 4-channel-wide region in the center of the array capable of providing a full view of all initially planned experiments.

Planning and efforts to expand the FMMS array began immediately following the restart of TREAT. An additional 96 detectors were evaluated, characterized, and prepared for installation at TREAT during the summer of 2018. Unfortunately, funding reductions forced the project towards a 5-year hiatus. In October of 2023 funding from the Department of Energy’s Nuclear Science User Facilities enabled the expansion to recommence. This report serves to document the activities performed to expand the FMMS detector array to 192 channels in order to provide a broader view of the larger and more sophisticated test capsules currently planned for future irradiation in the TREAT reactor. This expansion also included doubling the data acquisition capability, addressing the new heat load on the system, and synchronizing the time for all digital components.

### **FUEL MOTION MONITORING SYSTEM**

The FMMS is a unique instrument composed of an array of heavily collimated sensors that detect neutrons and gamma-rays emanating from an experimental capsule positioned in the center of the TREAT reactor during operation. Each collimated detector provides a position-limited view of emissions from a single region of a test geometry. These components are illustrated in Figure 1. Lead sheet components of the system are also shown in this figure that can be configured across the face of the detector array to reduce count rates to manageable levels for extremely high emission tests. The FMMS detectors are composed of proton-recoil scintillators coupled to photomultiplier tubes. A photograph of an individual FMMS detector is shown in Figure 2. While these detectors were initially designed to detect fast neutron interactions with a high level of insensitivity to the prodigious amounts of gamma-rays produced during transient conditions, modern digital data acquisition and analysis methods allow for the discrimination of neutron and gamma-ray interactions in the zinc sulfide detector material and provide information about the emission rates of both types of particles from the test capsule.

Through analysis of the data from the array of detectors, a real-time two-dimensional image may be reconstructed to show the location of the fuel and its movement over time. This information is critical for understanding the dynamics of fuel behavior under transient conditions and for validating computational models that predict fuel behavior. Since the TREAT restart, the FMMS

data has been crucial to inform the development of advanced fuels and materials that can withstand extreme conditions.

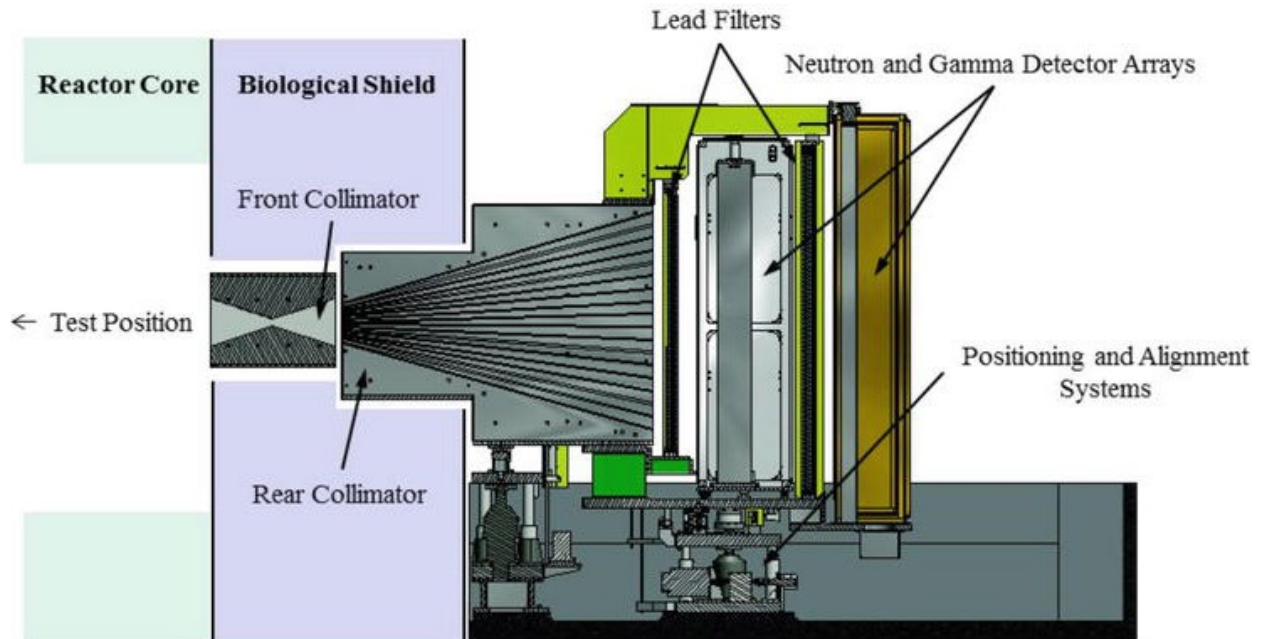


Figure 1. Cross-sectional illustration of the Fuel Motion Monitoring System components.



Figure 2. Hodoscope detector components including the proton recoil scintillator (in white) coupled to the photomultiplier tube.

## Heating Issues

During the seven years of operations of the original 96-channel array, the FMMS Data Acquisition System (DAQ) electronics have demonstrated high operational temperatures. Electronics operating at elevated temperatures can contribute noise to the signal and may cause reliability issues. Although the manufacturer of the DAQ electronics does not specifically identify a maximum operational temperature, they do indicate that elevated temperatures lead to accelerated deterioration. This behavior has also been observed by FMMS engineers who have

continually monitored hardware temperatures over the years and found a typical operational temperature of 154 °F.

As part of the plan for the expansion, the FMMS engineers identified that for optimal operation the hardware temperature should not exceed 130 °F. A TRIPP-LITE cooler was incorporated into the newly designed expansion chassis. The cooler was installed into the bottom of the rack such that cold air could be circulated by the system's fans. To further optimize the cooling of the chassis, various system component position configurations were tested. The wire mesh doors of the cabinet were found to play a significant role in allowing cool air to escape before being distributed by the system's fans. A Plexiglas cover was installed over the wire mesh door panels to prevent the cool air from escaping the system and help reduce the temperature of the entire cabinet. A photograph of the new cabinet and the cooler is shown in Figure 3. A log of the operational temperatures after the placement of the cooler is shown in Figure 4.



Figure 3. TRIPP-LITE cooler, shown on the left side, installed into the DAQ cabinet.

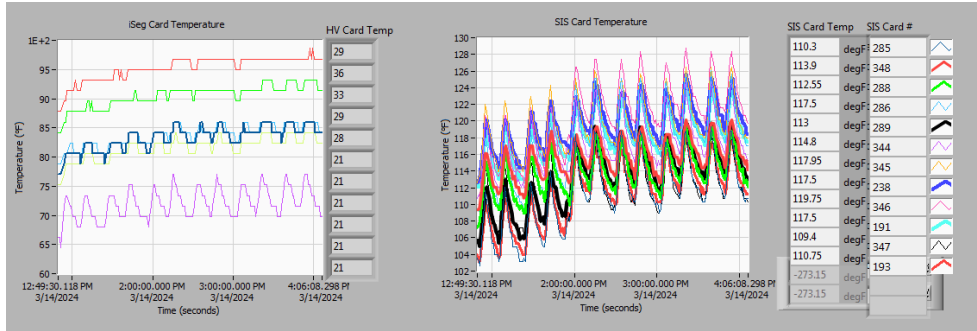


Figure 4. DAQ electronics temperatures after optimization of cooler placement. The centermost image demonstrates the cyclical cooling.

## Laboratory Testing

Detector assemblies were initially configured into a mock FMMS test cabinet located in INL's Applied Radiation Measurements and Systems Laboratory to enable testing with radiation sources prior to installation at TREAT. A photograph of this testing setup is shown in Figure 5. The specific detector locations were identified using 300-mm translation stages (Thorlabs, Inc.) to scan the entire area of the mock FMMS test cabinet. A  $Cf^{252}$  source with an emission rate of  $3.29 \times 10^6$  neutrons per second was used for this test. The scan parameters were set to 2.5-mm step resolution with a dwell time of 6 seconds resulting in a total scan time of four days. A photograph of the testing setup is shown in Figure 6 along with a plot of the detector locations.

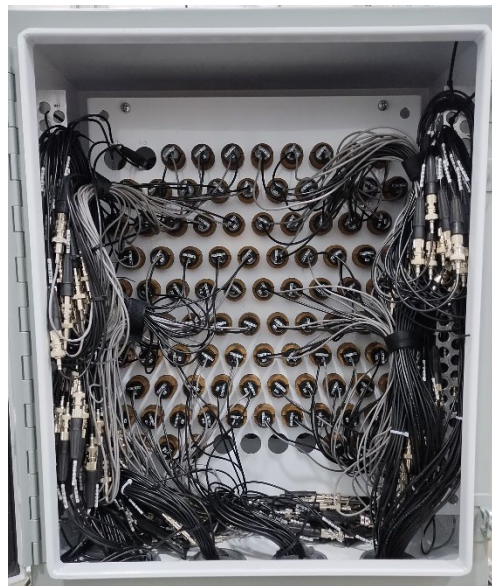


Figure 5. Mock FMMS testing cabinet.

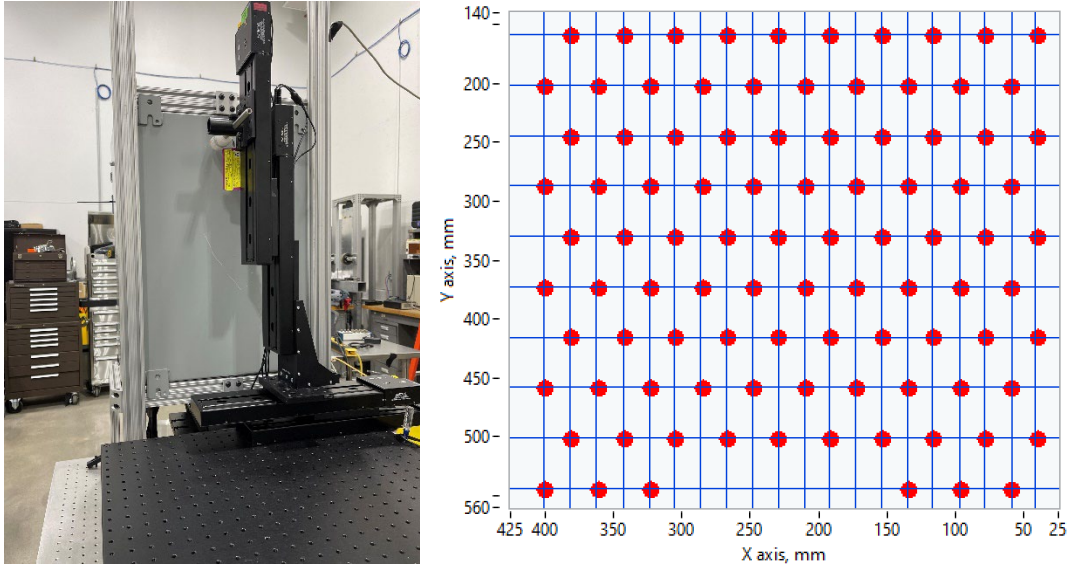


Figure 6. Scanning setup with translation stages and radioactive source (left) detector locations used in the mock FMMS testing cabinet (right).

## Voltage Bias

A voltage bias scan was performed to find the gain-response curve for each detector. This allowed the detectors to be set at a voltage that was appropriate for a specific count rate. The bias scan used five  $^{252}\text{Cf}$  sources approximately 20 inches away and at the center of the test stand that produced a cumulative emission rate of  $5.2 \times 10^6$  neutrons per second. The scan took place over 12 hours with a dwell time of 60 minutes for every 25-volt step over the bias range of -900 to -600 volts.

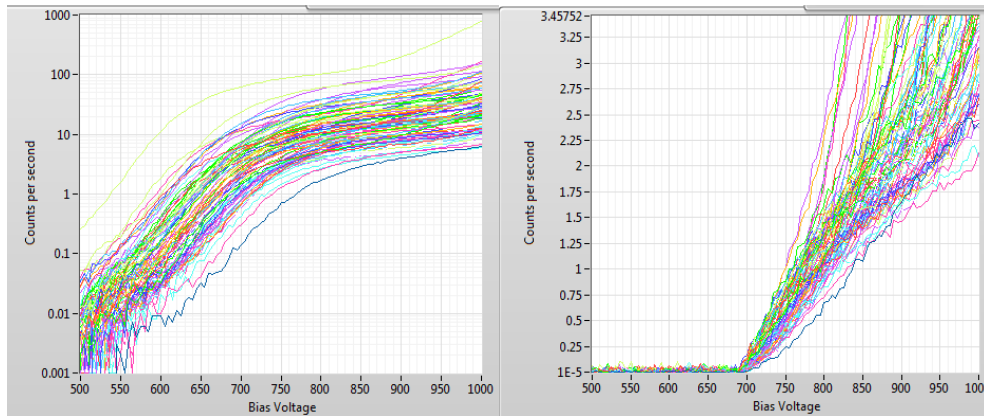


Figure 7. Results from the bias voltage scan (left). Minimum voltage values to power the detectors (right).

## Detector Count Rates

Detector count rates were measured by moving the Thorlabs stage to each detector location and counting for 30 seconds. The distance was set to 1/8" from the upright beam of the mock FMMS test stand; a photograph is shown in Figure 8. This offset was used to ensure that the

source holder was clear of obstructions as it moved to each detector location. The mean count rate from the normalization was 21.6 neutrons per second or an average absolute efficiency of  $4.15\text{E-}6$ .



Figure 8. Detector count rate measurement setup using five neutron sources.

A detector calibration was completed to normalize the count rate to 30 counts per second. This was automated using a proportional-integral-derivative (PID) controller to adjust the bias voltage until the count rate was within  $\pm 5\%$ . The mean count rate for all 96 detectors was 29.9 counts per second with a standard deviation of 0.57, correlating to an absolute sensitivity to spontaneous fission energy neutrons of  $5.74\text{E-}6$ . These results are shown in Figure 9. This same calibration was repeated with 39 spare detectors to allow for concurrent testing of the expanded data acquisition system (designed for 192 channels). The bias scan for all 135 detectors was completed using five  $^{252}\text{Cf}$  sources placed in the center and 10.5" from each of the 2 mock test stations. The scan parameters included a 5-minute dwell, with 25-volt steps from -600 to -1000 volts. The results are shown in Figure 10.

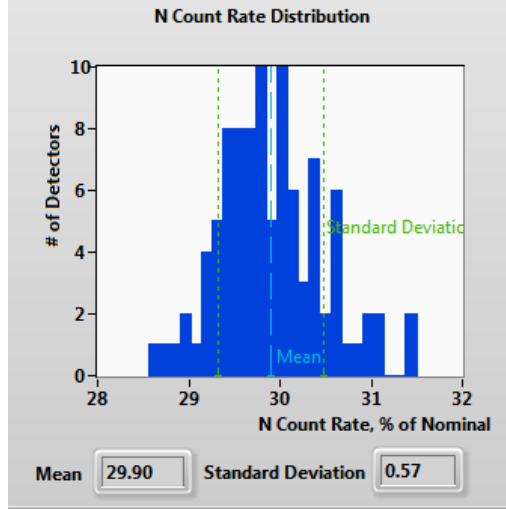


Figure 9. Total distribution of the source normalization

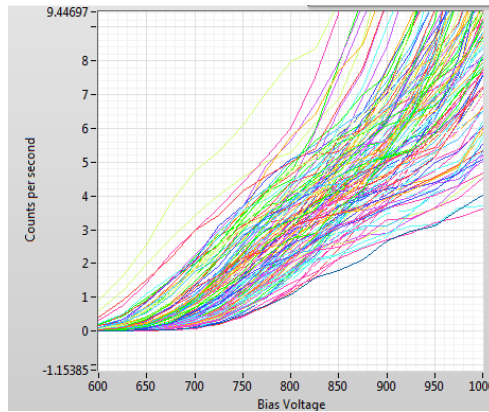


Figure 10. Voltage bias scan results for 135 detectors using the expanded acquisition system.

To continue evaluating the expanded acquisition system, a calibration scan was done to normalize the 135 detectors available during testing. This was completed using a 300 second dwell time and a targeted count rate of 40 counts per second with a tolerance of 2%. This scan resulted on a mean count rate of 39.96 with a standard deviation of 0.39, this distribution is shown in Figure 11. An observation was made that some of the pulse shape discrimination (PSD) distributions for some detectors were noisier than expected. A figure of merit (FOM) was calculated for each detector’s PSD distribution to provide a threshold performance value for further investigation and detector reassembly. The FOM (Equation 1) was calculated by summing the full-width at half-maximum (FWHM) of neutron and gamma-ray peaks in the PSD distribution and then dividing by the separation distance between the centroids of these peaks; this is illustrated in Figure 12. Examples of two vastly different FOM evaluations are shown in Figure 13. All detector assemblies with a FOM of less than one were pulled from the array for further investigation. Upon examination of these detectors, it was observed that the proton recoil scintillators (PRS) had become optically uncoupled from their corresponding photomultiplier tubes (PMT) in storage. These detectors were recoupled prior to installation at TREAT.

$$FOM = \frac{FWHM\ neutron + FWHM\ gamma}{Peak\ Separation} \quad (1)$$

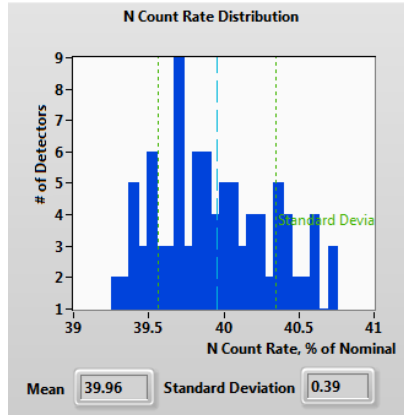


Figure 11. Count rate distribution after the automated normalization of the 135 detectors.

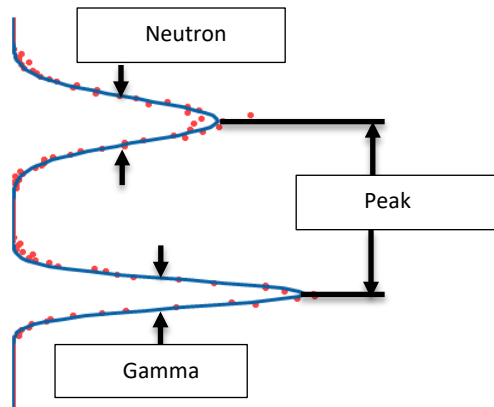


Figure 12. Illustration of the FOM components used in Eq. 1.

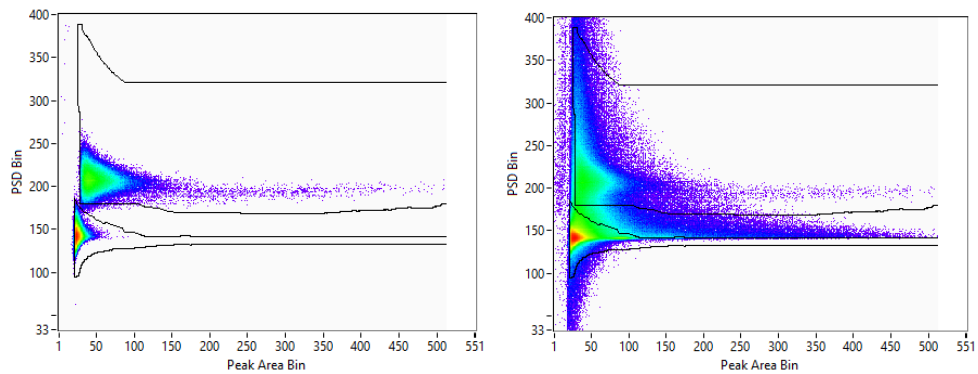


Figure 13. Detector Figure of Merit (FOM) examples: FOM greater than one (left) and FOM less than one (right).

## Efficiency Measurements

The neutron time-of-flight (ToF) method is a technique employed to ascertain the speed of neutrons, which in turn allows for the determination of their energy. In this process, the known energy distribution of neutrons emitted from  $^{252}\text{Cf}$  is utilized as a benchmark. By comparing this well-characterized distribution with the neutron energy distribution that is measured experimentally, it is possible to deduce the relative neutron efficiency. The measurement utilized a "start" stilbene detector, which triggered the start of a clock. The clock was then halted when an event was detected in any of the hodoscope detectors, this ToF spectrum is shown in Figure 14. The relative neutron efficiency results are shown in Figure 15. A standard PSD technique was also employed to distinguish between gamma-rays and neutrons as a comparison to this detection time discrimination. This technique capitalizes on the differences in the waveforms produced by the interactions of these particles with the detector material (i.e. neutron pulse shapes have longer tails than gamma pulses), see Figure 16.

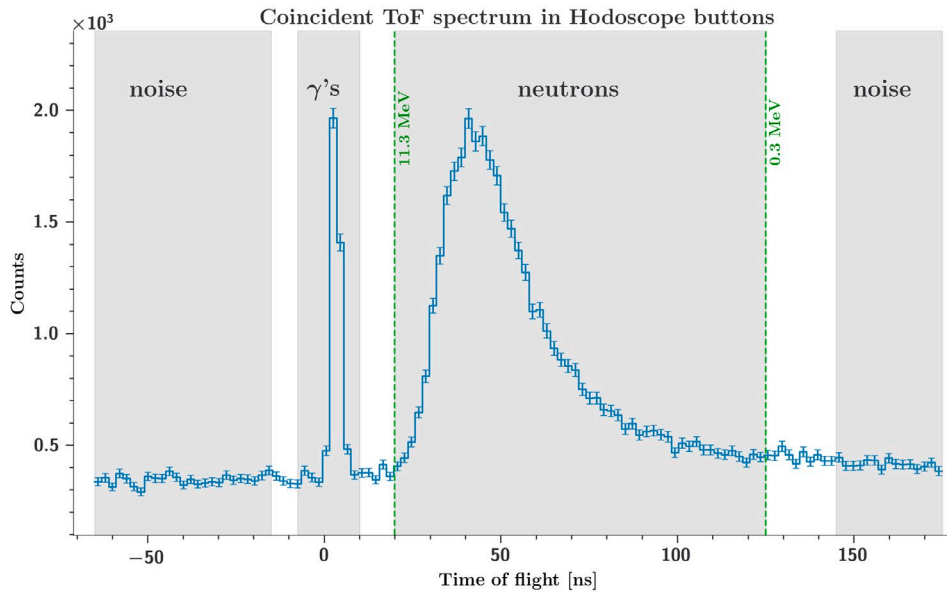


Figure 14. Example time of flight spectrum for a FMMS detector assembly.

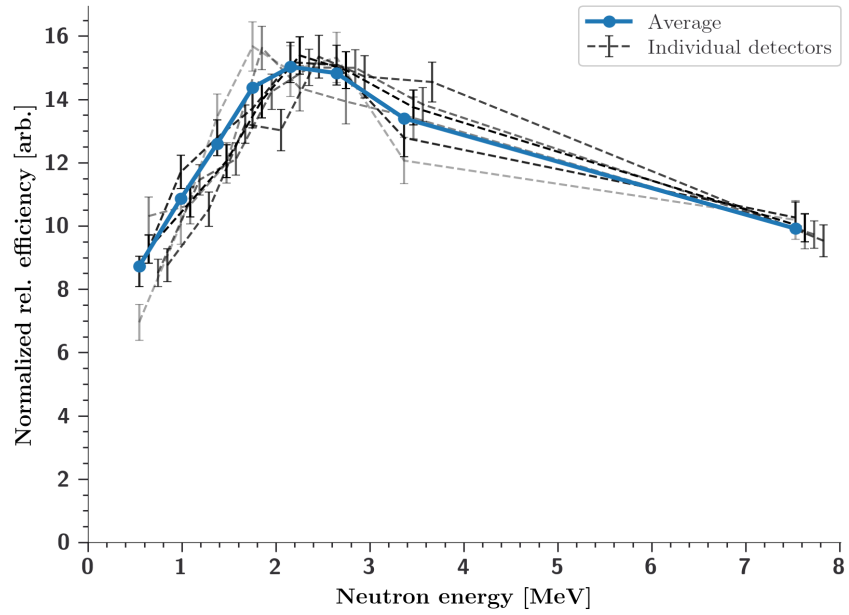


Figure 15. Relative neutron efficiency for the evaluated detectors.

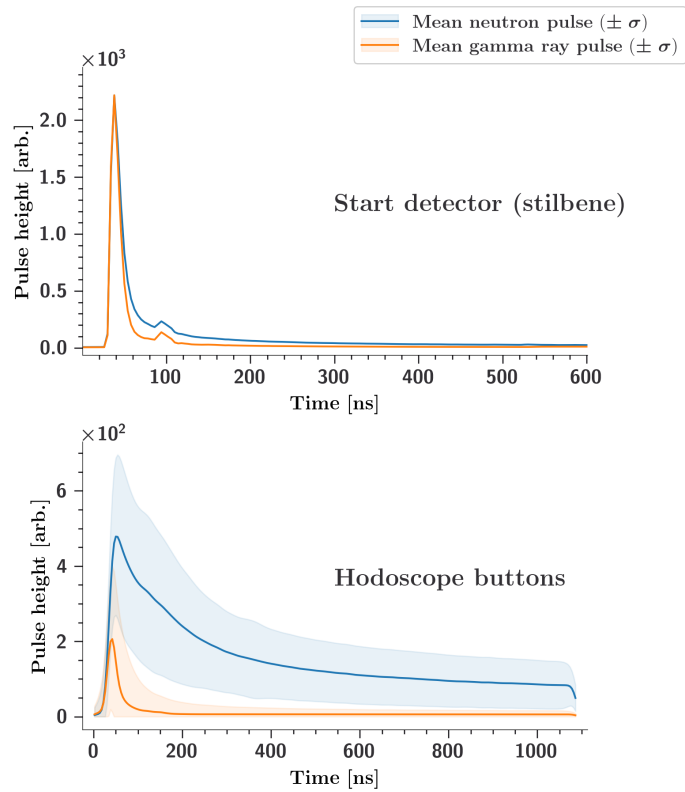


Figure 16. Mean pulse height comparison of hodoscope detectors and the start stilbene detector.

## Absolute Efficiency

To determine absolute efficiency, it is necessary to determine a scaling factor that can be applied to the relative efficiency measurements. The ToF method was not suitable for this purpose because it introduced an unknown scaling constants that could skew the results. To circumvent this issue, the detectors were operated without coincidence and gamma events were rejected using PSD. Despite these measures, the resulting absolute neutron detection efficiencies, shown in Figure 17, exhibited variance by up to approximately a factor of 2. These discrepancies could potentially be attributed to the degradation of the optical coupling between the scintillators and the photomultiplier tubes.

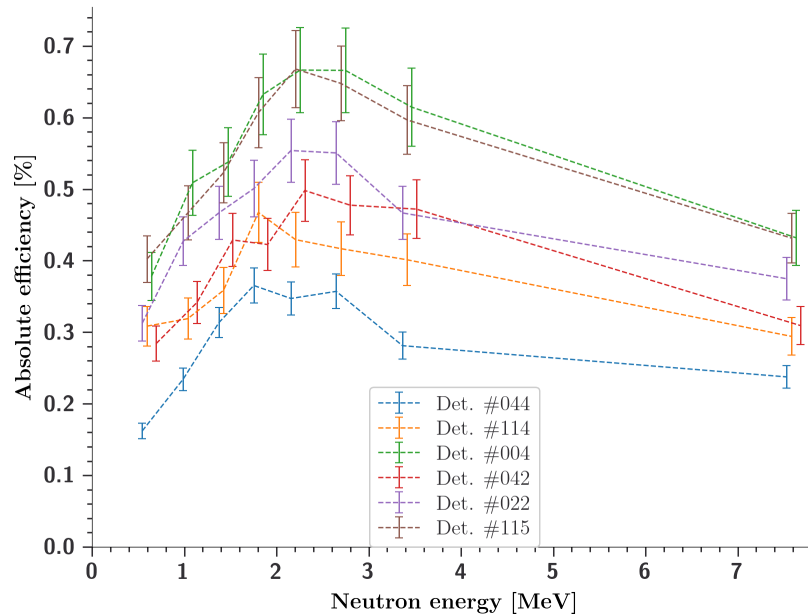


Figure 17. Absolute neutron efficiency for the five evaluated detectors.

## SYSTEM INSTALLATION

The FMMS expansion efforts took place the first week of June 2024. The process started with opening the FMMS cabinet and having radiological control survey for contamination. No contamination was found, allowing for the removal of all the original 96 detector assemblies. Concurrently, the placement of all 100-foot signal and voltages cables was conducted. Photographs of both activities are shown in Figure 18.

Discovery of various levels of detector uncoupling in laboratory testing prompted the team to inspect all currently installed detector components for anomalies such as separation between the scintillator and waveguide, cracks, and dried optical gel. After the inspection (shown in Figure 19), cleaning and recoupling of all the PRS and PMTs was completed applying new optical gel. Photographs of the clean components can be seen in Figure 20. All 192 detectors PSD were evaluated once more. A comparison of the FOM between the new 192 detectors and the original 96 FMMS detectors (prior to cleaning and recoupling) is shown in Figure 21. The FOM of the detectors in the 96 channel FMMS had significantly degraded since installation.



Figure 18. Disconnecting of the cables and removal of the detectors (left). Placement of the new 100-foot cables (right).



Figure 19. Visual inspection of PRS components

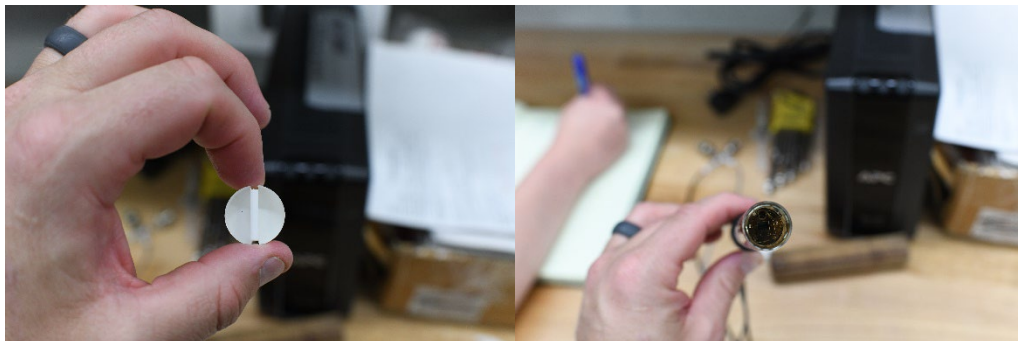


Figure 20. Photographs of clean PRS (left) and PMT (right) components.

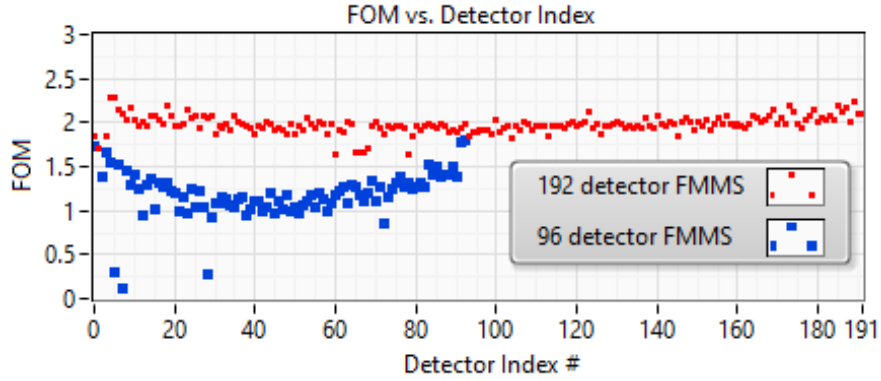


Figure 21. FOM comparison between the new 192 detectors and the original 96 FMMS detectors.

The newly recoupled detectors were inserted in their corresponding positions as illustrated in Figure 22. The new signal and high voltage cables were connected to all 192 detectors. A photograph of the connected detectors is shown in Figure 23. The rest of the cable length being placed in the trench, shown in Figure 24, leading to the FMMS data acquisition cabinet in a separate room. After all the detectors were installed and connected to the FMMS DAQ, a performance verification scan was conducted to ensure that no high voltage or signal cables were crossed during the installation process. A Plutonium-Beryllium (PuBe) source was used to scan in 10-mm increments with a dwell time of 60 seconds at each position, totaling over 200 hours. These results are shown in Figure 25.

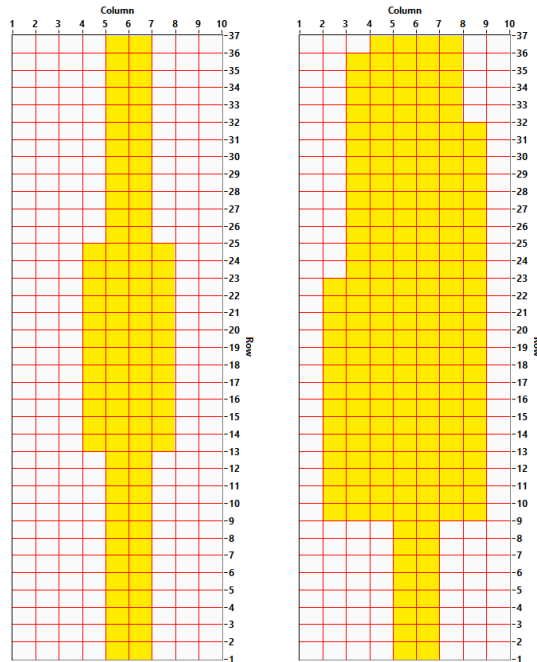


Figure 22. Comparison of the original FMMS coverage area (left) and the new (right).



Figure 23. Photograph of the new installed detectors connected to their respective cables.



Figure 24. Placement of signal and high voltage cables inside the trench.

The team proceeded to complete a base-line normalization using the same PuBe source positioned at each detector location. Automated adjustments were made to each detector's bias voltage to obtain a count rate of 40 counts per second with a 10% tolerance. The system's final mean count rate was 40.71 with a standard deviation of 1.64 or +/- 3.9%. These results are shown in Figure 25 and Figure 26.

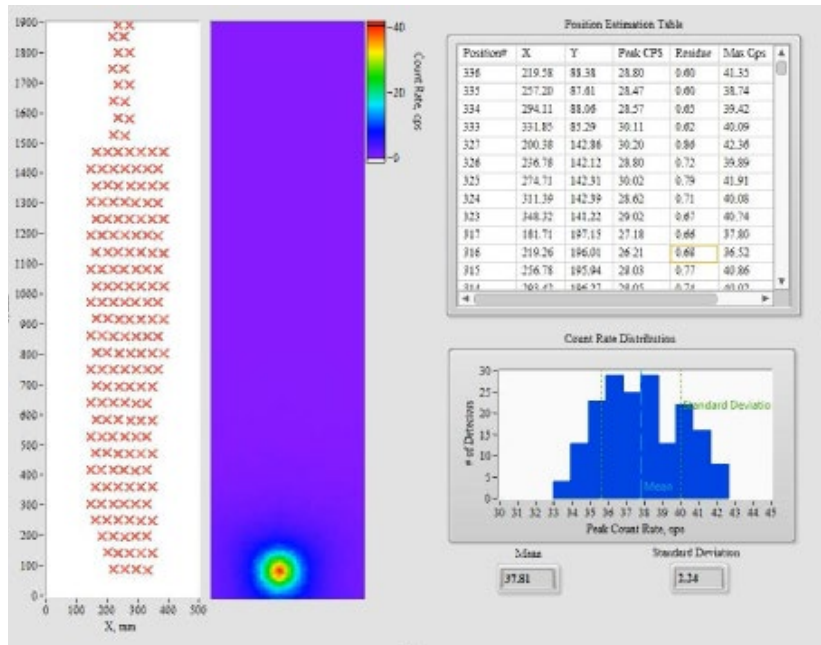


Figure 25. Verification scan with the new FMMS DAQ and new detectors.

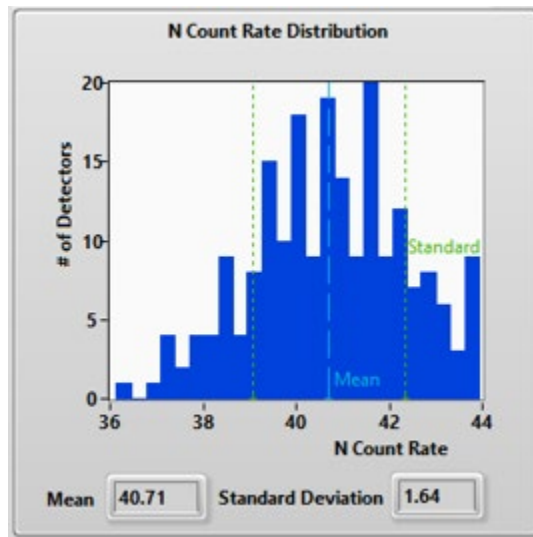


Figure 26. Neutron count rate distribution of the baseline scan using the new 192 detectors and DAQ.

An additional scan was completed to verify the set parameters for each detector, i.e. detector voltage, location, PSD map and detector number, were saved to the configuration correctly. This scan was completed with the same procedure as the previous normalization, but for a much longer dwell time of 1200 seconds at each detector position. When the verification scan was completed, the neutrons had a mean count rate of 53.60 and a standard deviation of 2.27. These results are shown in Figure 27.

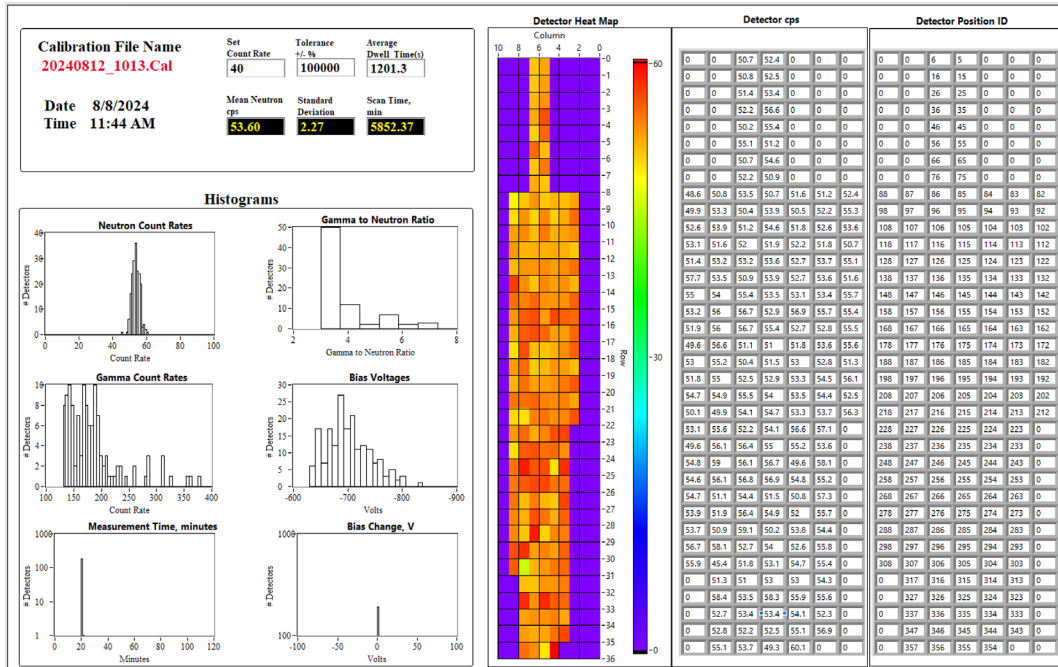


Figure 27. Results of the verification scan to verify each detector's parameters.

## Environmental Monitoring

An environmental monitoring system, RoomAlert32s (Actech, Inc.), was installed to monitor the DAQ chassis and FMMS room environment. The system has internal sensor which reads temperature, humidity, and dewpoint at the middle level of the chassis where the monitoring system was installed, see Figure 28. Two external sensors were connected to the system to record temperature and humidity at the top and bottom levels of the chassis. An set of switch sensors was installed to record the on/off state of various devices including the uninterrupted power supply connected to the FMMS DAQ chassis. Additional sensors were also configured to monitor the main power input and the airflow of the cooling system. All the data and information collected by the RoomAlert32s is sent to a LabVIEW program to be logged in real time and be visually displayed, a screenshot of the graphic user interface is shown in Figure 29. The program is configured to send alerts when the FMMS chassis is operating outside of optimal parameters.

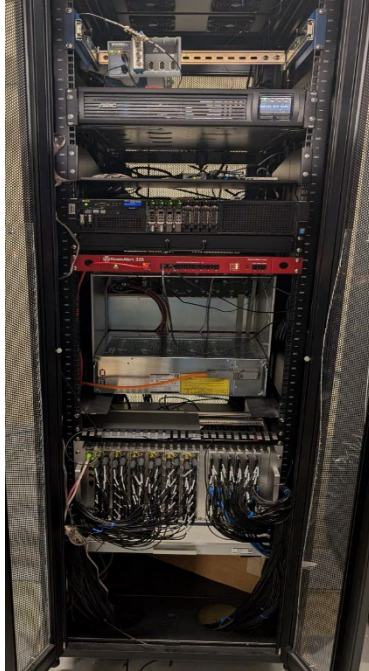


Figure 28. FMMS chassis with all new components, the environmental monitor hub (red) is located in the middle.



Figure 29. RoomAlert32S graphic user interface.

## SYSTEM TESTING

An operational test was performed with the TREAT reactor held at a constant 80 kW to enable the verification of detector performance. The FMMS and its detectors performed as expected and none of the high voltage values or lower-level discriminators required adjustment following this test. These results are shown in Figure 30.

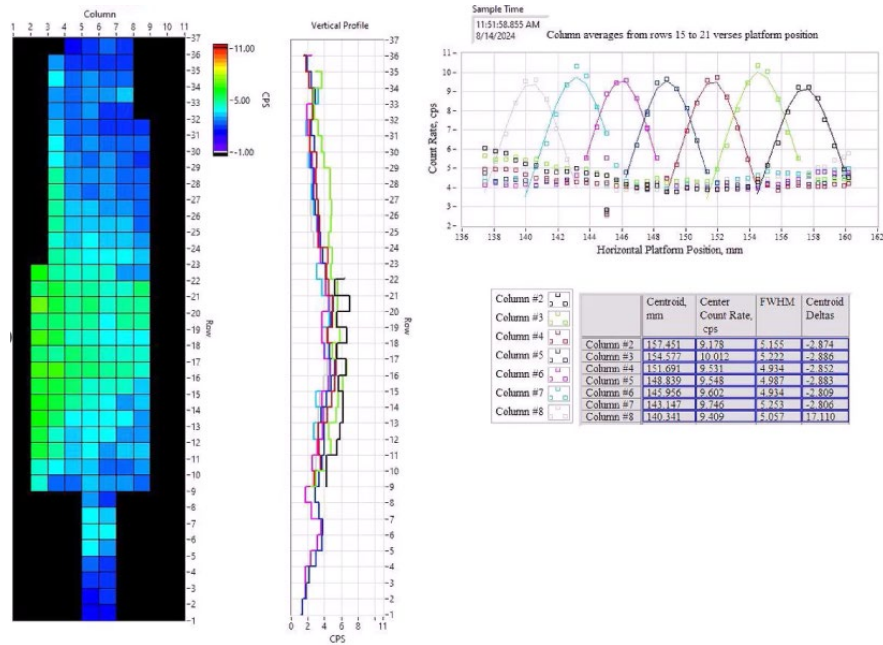


Figure 30. Cumulative number of counts after the 80 kW

## Data Acquisition Synchronized Timing

At the foundation of the FMMS DAQ is a collection of 16-channel struck digitizers that record perform preliminary analysis of collected detector signals. Each of these signal digitization cards is equipped with its own clock oscillator circuit that is fundamental for recording detection times during a measurement. However, these circuits are not identical and will inevitably experience drift, gradually losing synchronization with one-another over a prolonged acquisition time. An example of this drift is shown in Figure 31. This time drift has been quantified to be within a margin of  $\pm 1.0$  millisecond over a duration of 600 seconds (the typical measurement time for a transient test). While a deviation of a few milliseconds may seem marginal, equating to only a few bins throughout the course of a transient measurement, it gains significance in the context of longer duration experiments or prolonged system usage.

A new paradigm was introduced to the DAQ utilizing the front panel bus as opposed to the rear panel bus used for data transfer. A single card in the array is now designated as “master” and periodically provides a signal to the remaining cards for resynchronization. Establishing this mode of operation required a significant rewrite of the FMMS control software and extensive laboratory testing.

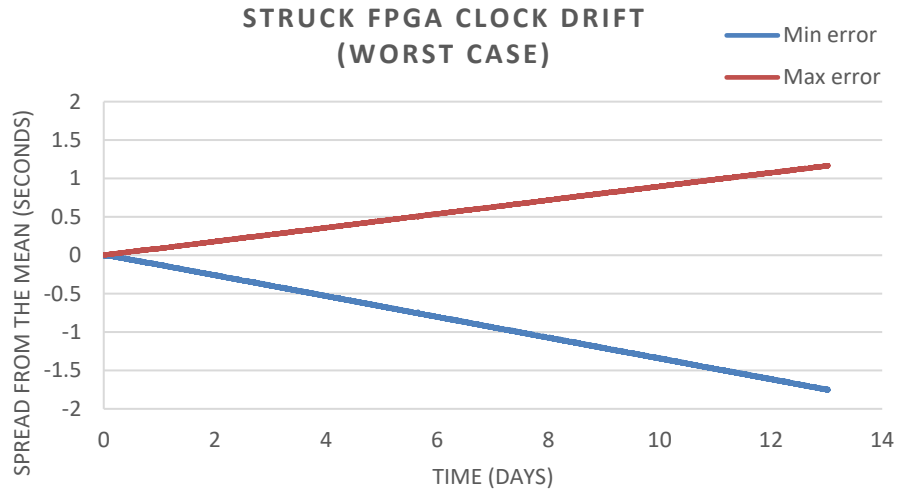


Figure 31. Example of Struck card drift over several days.

## Transient Reporting

Upon completion of a transient, a Transient Pulse Summary (TPS) Report is generated using the Fuel Motion Data Analysis and Reporting Code (FM DARCo). This report follows a format that segments the total transient time over four sequential sections aiming to illustrate what the FMMS is recording. The FM DARCo was updated to accommodate double the data which forced a rearrangement of the plotting configuration for the various figures. A sample TPS report is included in

## ACKNOWLEDGEMENTS

This expansion was made possible by the U.S. Department of Energy Office of Nuclear Energy's Nuclear Science User Facilities. TREAT facility staff were instrumental in every stage of the planning and execution of the FMMS upgrade effort. INL is operated for the U.S. Department of Energy by Battelle Energy Alliance under DOE contract DE-AC07-05-ID14517.

*Page intentionally left blank*

**Appendix A**

**Transient Pulse Summary Report**



# ***Transient Pulse Summary Report***

## **Fuel Motion Monitoring System**

**Transient number: 3171**

Experiment name: LOC-C-3-A  
Experiment date: 2024-08-15  
Experiment point of contact: C.B. Jensen

Prepared by: S. J. Thompson & L. A.  
Ocampo Giraldo

Distribution list: D. L. Chichester  
J. D. Hix  
T. V. Holschuh  
J. T. Johnson  
L. A. Ocampo Giraldo  
S. J. Thompson

# Transient Pulse Summary Report

## Fuel Motion Monitoring System

### Transient Information

<b>TRANSIENT NUMBER</b>	<b>3171</b>
<b>EXPERIMENT POINT OF CONTACT</b>	C.B. Jensen
<b>EXPERIMENT DATE</b>	2024-08-15
<b>EXPERIMENT TIME (MST/MDT)</b>	12:44 MDT TIME
<b>EXPERIMENT TIME (UTC)</b>	18:44 UTC TIME
<b>FMMS NUMBER OF LEAD SHEETS</b>	1 of 12 (1.25 cm)
<b>FMMS ACTIVE DETECTORS</b>	192
<b>DATE OF DETECTOR NORMALIZATION</b>	2024-08-07
<b>FMMS ENGINEER(S)</b>	J. T. Johnson & J. D. Hix
<b>FMMS SCIENTIST(S)</b>	S. J. Thompson & L. A. Ocampo Giraldo
<b>FMMS PRINCIPAL INVESTIGATOR</b>	D. L. Chichester
<b>COMMENTS</b>	None

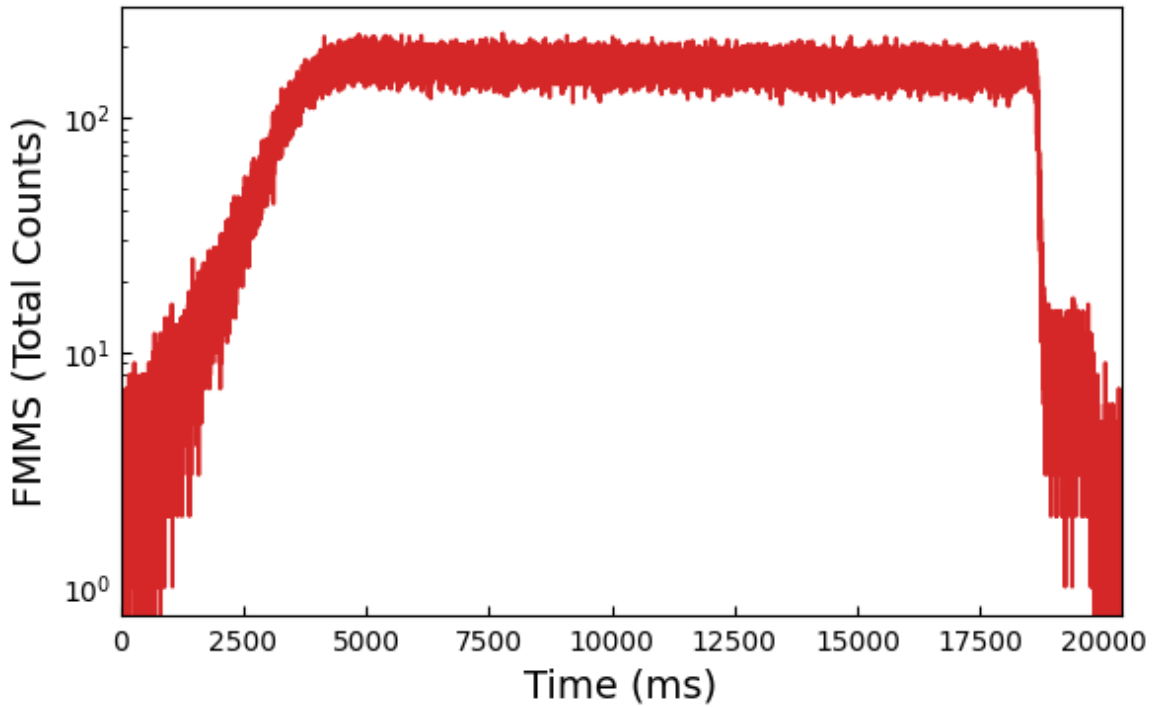


Figure 1. Profile of total detector counts over the duration of the transient.

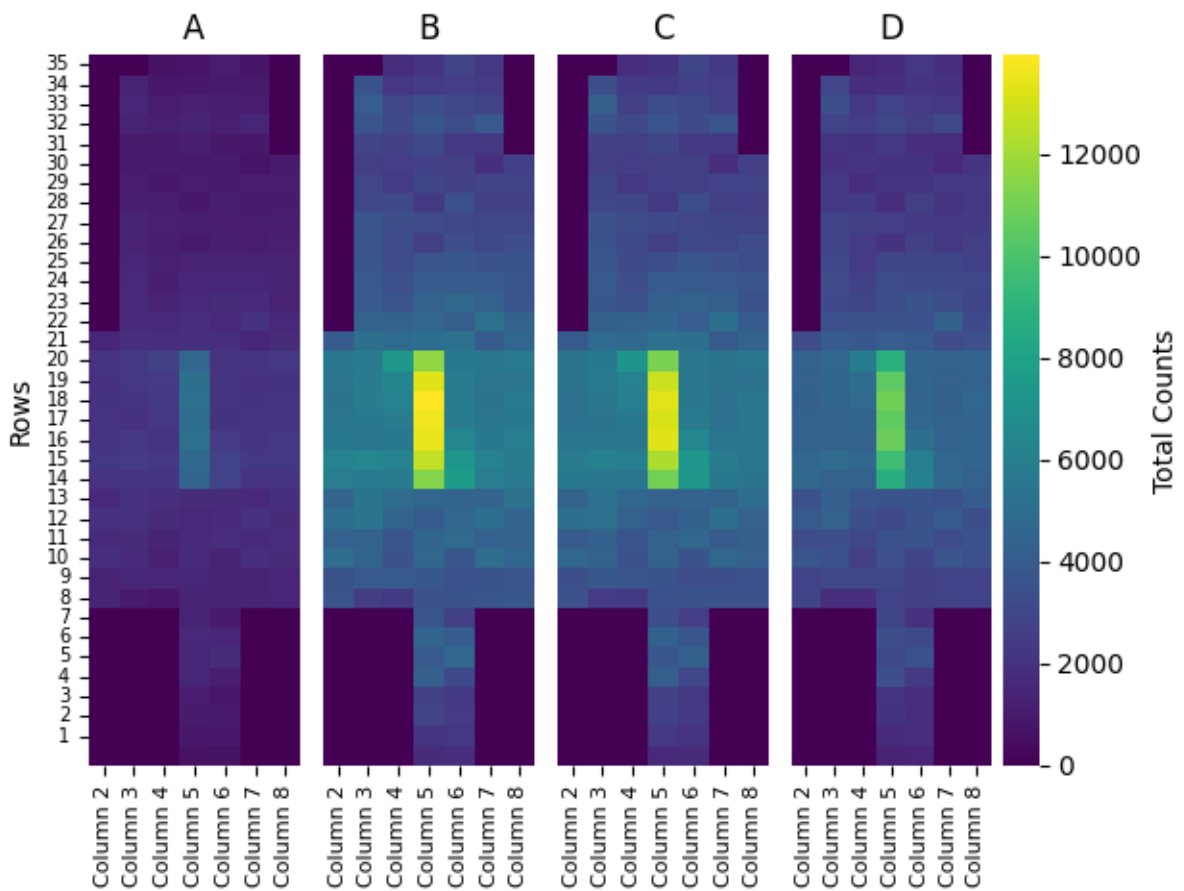
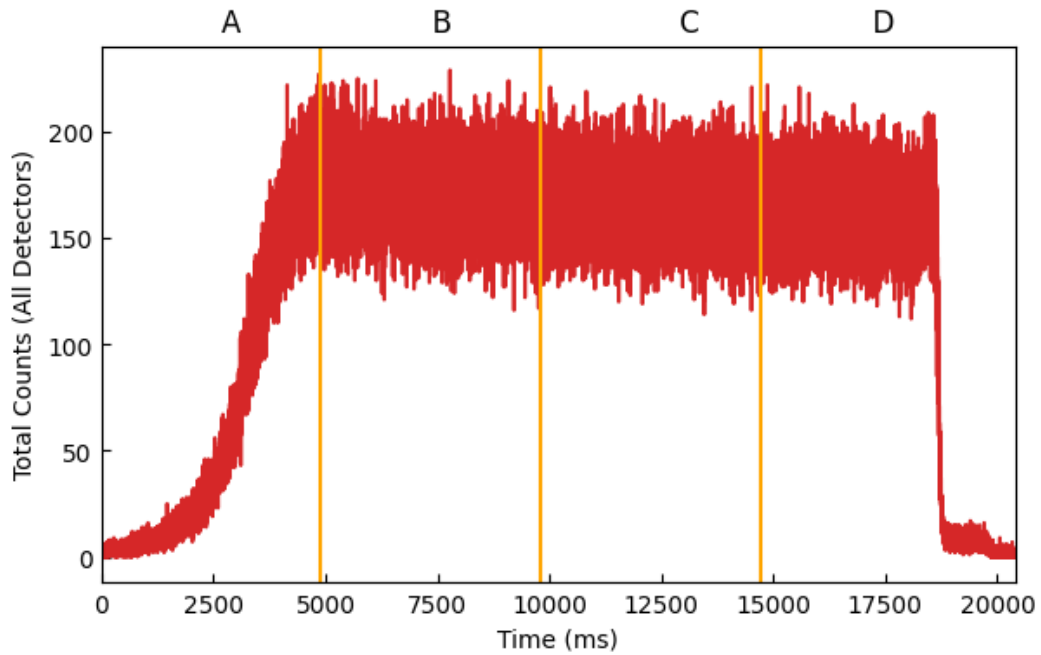


Figure 2. Profile of the total detector counts over the duration of the transient divided into four time sections, A through D (Above). Snapshots of the FMMS data central view during the four time sections (Below).

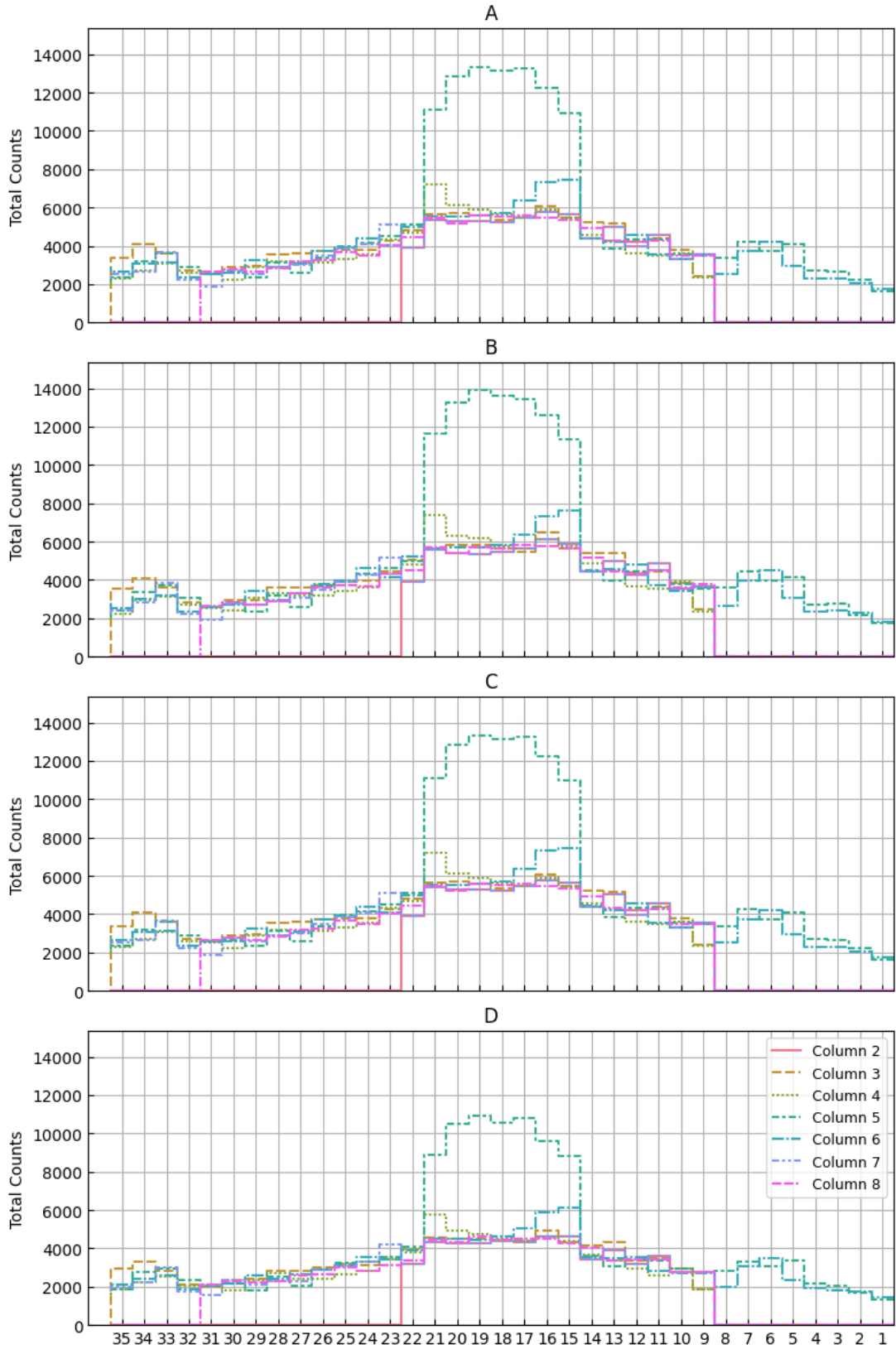


Figure 3. Vertical profile for the central columns of the FMMS core during time sections A-D of the transient.

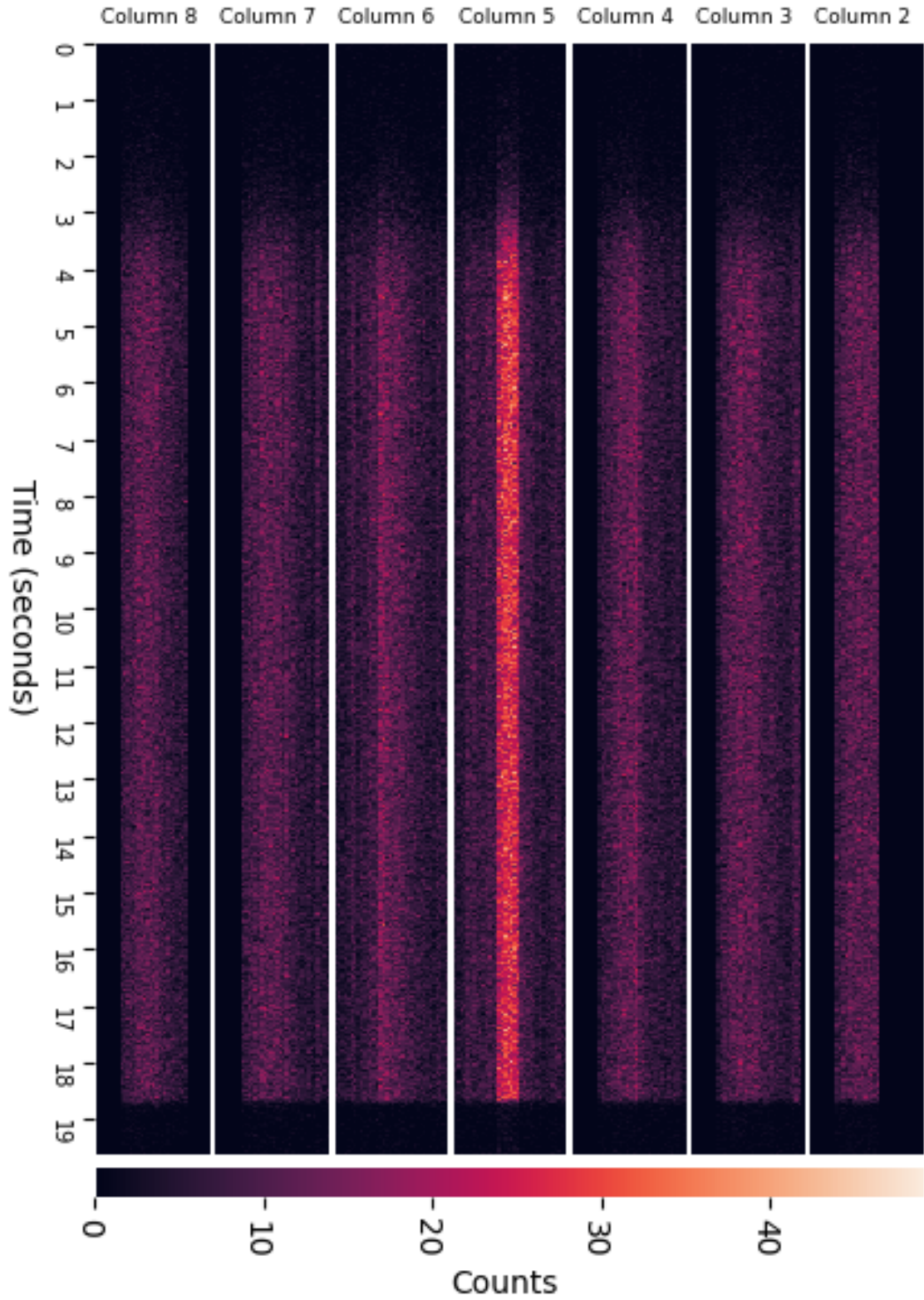


Figure 4. Waterfall plot of all FMMS detectors over the duration of the transient. The color scale in this image is on a linear scale.

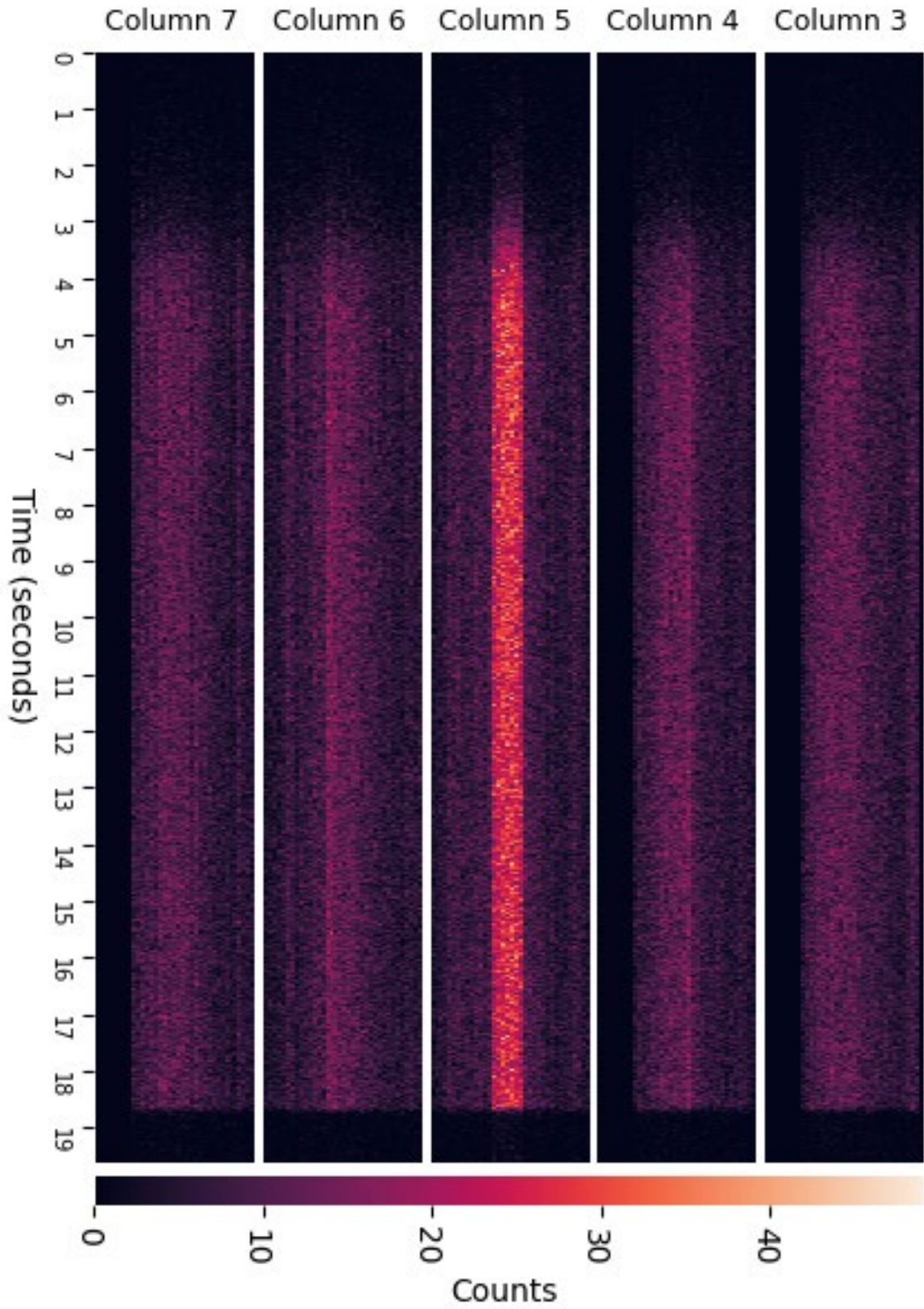


Figure 5. Waterfall plot of the center columns of the FMMS over the duration of the transient. The color scale in this image is on a linear scale.

